CDF note 7129

Version 1.0

Search for electroweak single-top-quark production in $p\bar{p}$ collisions at 1.96 TeV

(CDF collaboration)

(Dated: August 5, 2004)

Abstract

We report on a search for Standard Model (SM) electroweak single-top-quark production using $W + 2$ jets events in $p\bar{p}$ collisions at a center-of-mass energy of 1.96 TeV. Using a data sample of (162 ± 10) pb^{-1} recorded by the upgraded Collider Detector at Fermilab (CDF) we search for a signal of t-channel (Wg-fusion) and s-channel (W^*) single-top production as well as a combined signal of the two processes. We find no evidence of a single-top-quark signal and thus set upper limits on the production cross section: 10.1 pb (5.1 times the SM prediction) for the t-channel, 13.6 pb (15.4 times the SM prediction) for the s-channel and 17.8 pb (6.2 times the SM prediction) for the combined cross-section of t- and s-channel.

PACS numbers: 14.65.Ha, 12.15.Ji, 13.85.Rm, 87.18.Sn

In $p\bar{p}$ collisions at 1.96 TeV top quarks are predominantly produced in pairs via strong interaction processes. However, within the Standard Model (SM) top quarks are also expected to be produced singly by the electroweak interaction involving a W-t-b vertex [1, 2]. For the Tevatron two production modes are relevant: production via the t- or s-channel exchange of a virtual W-boson, also referred to as Wg-fusion or W^* process, respectively. Representative Feynman diagrams are shown in Fig. 1. The measurement of single-top events is particularly interesting because the production cross-section is proportional to $|V_{tb}|^2$, where V_{tb} is the Cabibbo-Kobayashi-Maskawa (CKM) matrix element which relates top- and bottom-quarks. Assuming three quark generations, the unitarity of the CKM matrix implies that V_{tb} is close to unity [3]. In this assumption ($|V_{tb}| = 1$), the most recent next-to-leading order calculations predict cross-sections of (1.98 ± 0.25) pb for the t-channel and (0.88 ± 0.11) pb for the s-channel mode at $\sqrt{s} = 1.96$ TeV [4, 5] (The cross-section uncertainties include PDF, top-quark mass and factorization scale uncertainties.). When related to these predictions, a measurement of the single-top cross-section would allow to directly measure $|V_{tb}|$. If there are more than three generations, V_{tb} is essentially unconstrained by theory, and measuring the single-top cross-section represents the only window for directly probing the W-t-b coupling. Furthermore, single-top searches test various models which predict anomalously altered single-top production rates [6]. Using Tevatron Run I data taken in 1992 – 1995 the CDF collaboration reported upper limits on the production cross-section for single top events at 95% confidence level (C.L.): 13 pb for the t-channel (i.e. 9.0 times the SM prediction at $\sqrt{s} = 1.8$ TeV), 18 pb for the s-channel (i.e. 23.7 times the SM prediction at $\sqrt{s} = 1.8$ TeV) and 14 pb for the combined cross-section (6.4 times the SM prediction) [7].

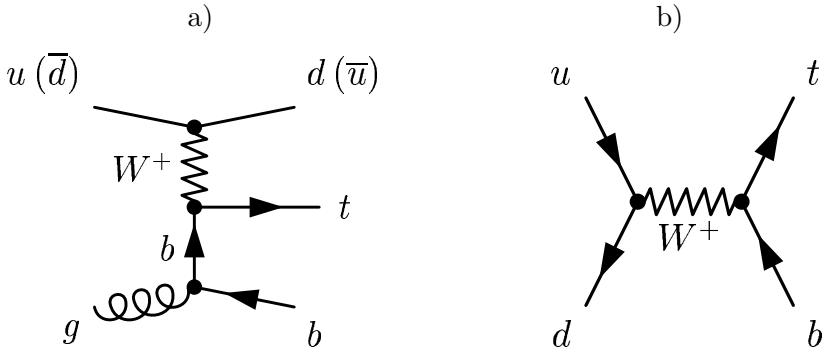

FIG. 1: Feynman diagrams for single-top production: a) t-channel (Wg), b) s-channel (W^*).

A more recent, optimized single-top search for the combined s- and t-channels found a small signal excess and a 95% C.L. limit of 24 pb [8]. The DØ collaboration has published upper limits on single-top production in Run I of 22 pb on the t-channel and 17 pb on the s-channel mode at 95% C.L. [9].

The experimental signature of single-top events consists of the W decay products plus two or three jets, including one b-quark jet from the decay of the top quark. To suppress QCD multi-jet background we select only the decays $W \to \mu\nu_\mu$ and $W \to e\nu_e$. We do not specifically consider the $W \to \tau\nu_\tau$ channel because of the large background associated with the hadronic decays of τ leptons. In s-channel (W^*) events we expect a second b-quark jet from the W-t-b vertex. In t-channel (Wg-fusion) events a second jet originates from the recoiling light quark and a third jet is produced through the splitting of the initial-state gluon into a $b\bar{b}$ pair, see Fig. 1. In most cases this second b-quark jet escapes detection, since it is produced at high values of pseudo-rapidity,$|\eta|$, and low transverse energy, E_T.

This article describes a search for electroweak single-top-quark production using a data sample from Run II of the Tevatron with the upgraded Collider Detector at Fermilab (CDF II). The data sample corresponds to an integrated luminosity of $(162 \pm 10)\,\mathrm{pb}^{-1}$. We perform two analysis: (1) a combined search, where we combine t- and s-channel to one single-top signal, (2) a separate search, where we try to determine the signal rate for the two single-top processes individually. Since the two single-top production modes have very different sensitivity to physics processes beyond the SM, it is important to isolate events of the two processes and measure the respective cross-sections separately [6]. This motivates the t-channel search.

The CDF II experiment is an azimuthally and forward-backward symmetric apparatus designed to study $p\bar{p}$ collisions at the Tevatron [10]. The inner part of CDF is dedicated to reconstruct the trajectories of charged particles and measure their momenta. The entire tracking volume is immersed into a solenoidal magnetic field of $|\vec{B}| = 1.4$ T. A silicon microstrip detector provides tracking over the radial range of 1.5 to 28 cm. A 3.1 m long open-cell drift chamber covers the radial range from 40 to 137 cm. The silicon detector fully covers the pseudo-rapidity region of $|\eta| \leq 2.0$, the drift chamber provides coverage up to $|\eta| \simeq 1.0$. Segmented electromagnetic and hadronic sampling calorimeters surround the tracking system and measure the energy flow of interacting particles in the pseudo-rapidity range of $|\eta| \leq 3.6$. This analysis uses the calorimeters to identify jets in the range

of $|\eta| \leq 2.8$. A set of drift chambers located outside the central hadron calorimeters and another set behind a 60 cm iron shield detect energy deposition from muon candidates with $|\eta| \leq 0.6$. Additional drift chambers and scintillation counters detect muons in the region $0.6 \leq |\eta| \leq 1.0$. Gas Cerenkov counters located in the $3.7 \leq |\eta| \leq 4.7$ region measure the average number of inelastic $p\bar{p}$ collisions per bunch crossing and thereby determine the instantaneous luminosity [11].

Our event pre-selection resembles very closely the selection used in the CDF measurement of the $t\bar{t}$ cross-section in the lepton+jets channel [12]. We accept events with evidence for a leptonic W decay: an isolated central electron or muon candidate with transverse energy $E_T > 20$ GeV or transverse momentum $p_T > 20$ GeV/c, respectively, and missing transverse energy $\not\!\!E_T > 20$ GeV from the neutrino. An electron or muon is considered isolated if the non-lepton E_T in an η-ϕ cone of radius 0.4 centered on the lepton is less than 10% of the lepton E_T or p_T. Muons and electrons are required to meet strict (*tight*) identification criteria. To remove di-lepton events from $t\bar{t}$-production and leptonic Z-boson decays, we accept only events with one and only one tight lepton. In addition, we veto events, if we find a second, loosely identified lepton candidate, that forms an invariant mass with the primary lepton between $76 < M_{\ell\ell} < 106$ GeV/c^2. Events in which the tight muon is consistent with a cosmic ray passing through the detector are rejected. Moreover, we veto electron events that are compatible with being conversions of high-E_T photons. We count jets with transverse energy $E_T \geq 15$ GeV and $|\eta| \leq 2.8$. The pseudo-rapidity range deviates from the standard jet counting applied in the $t\bar{t}$ cross-section measurement in the lepton+jets channel ($|\eta| \leq 2.0$), in order to increase the acceptance for t-channel single-top events by roughly 30%. Based on this jet definition the largest signal fraction is contained in the $W + 2$ jets bin and we obtain the best signal-to-background ratio if we restrict our analysis to W+2 jets events. At least one of these jets must be identified as likely to contain a b-quark (b-tag). The b-tagging relies on the reconstruction of displaced secondary vertices with the silicon microstrip detector. Secondary vertices with a transverse decay length significance ($\Delta L_{xy}/\sigma_{xy}$) above 3 are accepted as a b-tag for jets. For consistency we require that the charged lepton z_0 is within a window of 5 cm around the primary vertex used for b-tagging.

To further suppress background and improve our sensitivity, we apply a cut on the reconstructed invariant mass $M_{\ell\nu b}$ of the charged lepton, the neutrino and the b-quark jet: $140 \leq M_{\ell\nu b} \leq 210$ GeV/c^2. Fig. 3a shows the $M_{\ell\nu b}$ distribution for Monte Carlo samples

TABLE I: Event detection efficiencies for single-top separate and combined search.

Process	Event detection efficiency in %		
	Combined Search	Separate Search	
		1-tag-bin	double-tag-bin
t-channel	0.89 ± 0.07	0.86 ± 0.07	0.007 ± 0.002
s-channel	1.06 ± 0.08	0.78 ± 0.06	0.23 ± 0.02

and the mass window cut which was optimized at the 5 GeV level. For top-quark events this quantity resembles the top-quark mass. The transverse momentum of the neutrino is set equal to the missing transverse energy vector $\vec{\not\!\!E}_T$; the longitudinal component $p_z(\nu)$ is obtained up to a two-fold ambiguity from the constraint $M_{\ell\nu} = M_W$. Out of the two solutions we pick the more central (lower $|\eta|$ value) one. If the $p_z(\nu)$ solution has non-zero imaginary part as a consequence of resolution effects in measuring jet energies, we use only the real part of $p_z(\nu)$. If there are two b-tagged jets in an event, we pick the b-jet that has maximum $Q \cdot \eta$ to be used for top-quark reconstruction. Here Q is the charge of the tight lepton in units of the elementary charge e and η is the pseudo-rapidity of the b-jet. For the separate search only, we apply two additional cuts: (1) we subdivide the sample into events with one and only one b-tagged jet (1-tag-bin) and exactly two b-tagged jets (double-tag-bin); (2) for the 1-tag-bin we impose a higher threshold requirement on the leading (highest transverse energy) jet and require $E_T(\text{jet } 1) \geq 30$ GeV.

We determine the total event detection efficiency ϵ_{evt} for the signal from events generated by the MadEvent Monte Carlo program [13], followed by parton showering using PYTHIA [14] and then subjected to a full CDF II detector simulation. For t-channel single-top production we generated two samples, one $b + q \rightarrow t + q'$ and one $g + q \rightarrow t + \bar{b} + q'$ which we merged together to reproduce the p_T spectrum of the $\bar{b}$ as expected from NLO differential cross-section calculations. This is an improved model compared to the Pythia modelling used in the Run I analyses. ϵ_{evt} includes the kinematic acceptance, branching ratios, lepton and b-jet identification as well as trigger efficiencies. The numerical values of ϵ_{evt} for signal events are given in Tab. I. The acceptances for the separate search illustrate that the division into two b-tag-bins yields an additional distinction between the two single-top production processes. The largest contribution to the acceptance uncertainty

comes from the b-jet identification efficiency with a relative uncertainty of 7%. Combining these acceptances with the cross-sections predicted by theory and the integrated luminosity of our data sample we expect to see 4.3 ± 0.6 signal events in the combined search (t- plus s-channel) and 2.7 ± 0.4 t-channel events in the 1-tag-bin of the separate search. The number of expected signal events is summarized in Tab. II.

We distinguish two background components: $t\bar{t}$ events and non-top background. We estimate the $t\bar{t}$ background based on events generated with Pythia [14], normalizing to the theoretically predicted cross-section of $\sigma(t\bar{t}) = 6.70^{+0.71}_{-0.88}$ pb [15]. The resulting number of expected $t\bar{t}$ events are given in Tab. II; the uncertainties include theoretical and acceptance contributions. The non-top background consists of several components. The primary source ($\approx 62\%$) are the W+heavy flavor processes $\bar{q}q' \to Wg$ with $g \to b\bar{b}$ or $g \to c\bar{c}$ and $gq \to Wc$. Additional sources are "mistags" ($\approx 25\%$), in which a light-quark jet is erroneously identified as heavy flavor, "non-W"($\approx$ 10%), e.g. direct $b\bar{b}$ production, and di-boson production ($\approx 3\%$), which includes WW, WZ and ZZ production. The mistag and non-W rates are estimated using CDF II data. The W+heavy flavor rates are extracted from Alpgen [16] Monte Carlo events normalized to data and the di-boson rates from Monte Carlo normalized to theory predictions [17]. The total non-top background expectation is 30.0 ± 5.8 for the combined t- and s-channel search and 23.3 ± 4.6 for the separate search (1-tag-bin only). The expectations of signal and background rates are summarized in Table II. After all selection cuts we observe 42 events for the combined search, 33 events in the 1-tag-bin and 6 events in the double-tag-bin of the separate search. Within the errors the observations are in good agreement with expectations.

To extract the signal content in the two samples of candidate events we use a maximum likelihood technique for both the separate and the combined t- plus s-channel search. In the following paragraph we will describe the likelihood function for the separate search; the combined search uses an analogous definition. The most prominent difference in kinematics between t- and s-channel events occurs in the variable $Q \cdot \eta$, where Q is the charge of the tight lepton in the event, essentially tagging the flavor of the top quark, and η is the pseudo-rapidity of the jet which is not identified as a b-quark jet. The $Q \cdot \eta$ distribution exhibits a distinct asymmetry for t-channel events, while it is rather symmetric for other processes, as can be seen in Fig. 2a. In Fig. 2b we show the data versus stacked Monte Carlo templates weighted by the number of expected events. The separate search defines a

TABLE II: Expected number of signal and background events passing all selection cuts in the W+2 jets data sample for (162 ± 10) pb^{-1} of CDF II data, compared with observations.

Process	N events in combined search	N events in separate search	
		1-b-tag-bin	double-tag-bin
$t\bar{t}$ ($\sigma = 6.70^{+0.71}_{-0.88}$ pb)	3.8 ± 0.9	3.2 ± 0.7	0.60 ± 0.14
non-top	30.0 ± 5.8	23.3 ± 4.6	2.59 ± 0.71
Sum Background	33.8 ± 5.9	26.5 ± 4.7	3.19 ± 0.72
t-channel ($\sigma = 1.98 \pm 0.26$ pb)	2.8 ± 0.5	2.7 ± 0.4	0.02 ± 0.01
s-channel ($\sigma = 0.88 \pm 0.11$ pb)	1.5 ± 0.2	1.1 ± 0.2	0.32 ± 0.05
Sum Single-Top	4.3 ± 0.5	3.8 ± 0.5	0.34 ± 0.05
Sum Expected	38.1 ± 5.9	30.3 ± 4.7	3.53 ± 0.72
Observed	42	33	6

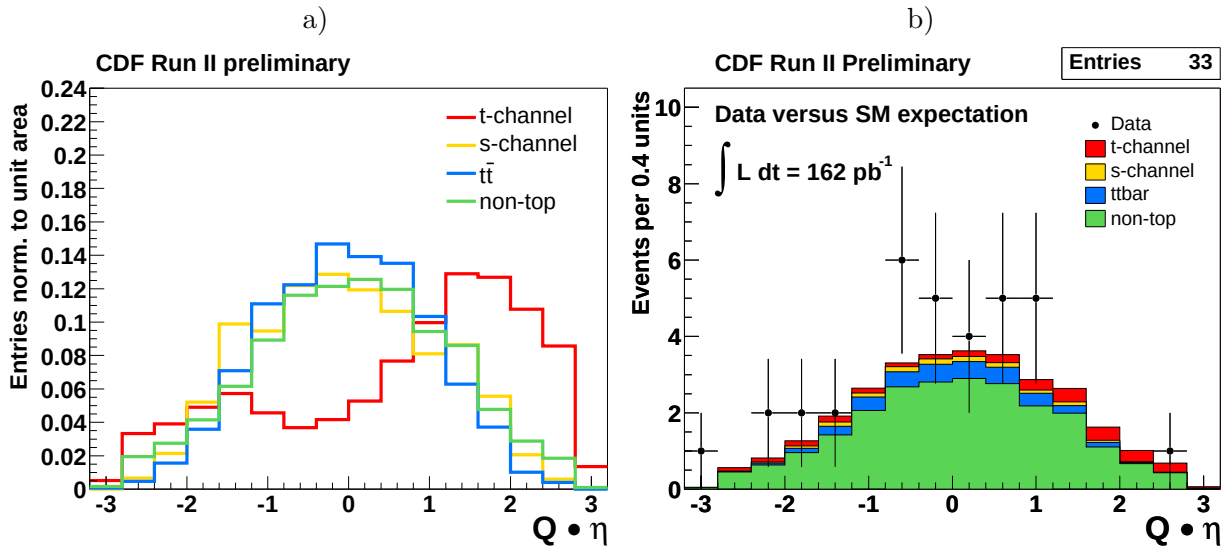

FIG. 2: $Q \cdot \eta$ distributions. a) Monte Carlo templates normalized to unit area. b) data in the 1-b-tag-bin (33 events) versus stacked Monte Carlo templates normalized to the SM expectation.

joint binned maximum likelihood for the $Q \cdot \eta$ distribution in the 1-tag-bin and the number of events in the double-tag-bin. Four signal and background processes are considered and numbered by the index j: $j = 1$: t-channel, $j = 2$: s-channel, $j = 3$: $t\bar{t}$ and $j = 4$: non-top. The cross-sections σ_j enter as normalized parameters $\beta_j = \sigma_j/\sigma_{SM,j}$ in the likelihood

TABLE III: Systematic acceptance uncertainties ϵ_{ij+} and ϵ_{ij-} for t- and s-channel single-top, the combined signal and the backgrounds.

		Separate Search		Combined Search
No.	Source	t-channel	s-channel	t- and s-channel
1	Jet energy scale	$^{+2.4}_{-6.7}\%$	$^{+0.4}_{-3.1}\%$	$^{+0.1}_{-4.3}\%$
2	ISR	$\pm 1.0\%$	$\pm 0.6\%$	$\pm 1.0\%$
3	FSR	$\pm 2.2\%$	$\pm 5.3\%$	$\pm 2.6\%$
4	PDF	$\pm 4.4\%$	$\pm 2.5\%$	$\pm 3.8\%$
5	Generator	$\pm 5\%$	$\pm 2\%$	$\pm 3\%$
6	Top quark mass	$^{+0.7}_{-6.9}\%$	-2.3%	-4.4%
7	ϵ_{trig}, ϵ_{ID}, luminosity	$\pm 9.8\%$	$\pm 9.8\%$	$\pm 9.8\%$

function. The normalization is with respect to the Standard Model expectation $\sigma_{SM,j}$. The β_j of the backgrounds are constrained by Gaussian priors $G(\beta_j, 1.0, \Delta_j)$. The cross-section uncertainties Δ_j are 13% for the two single-top processes, $\Delta_3 = 23\%$ for $t\bar{t}$ and $\Delta_4 = 20\%$ for the non-top background. Systematic uncertainties are parametrized and included in the likelihood definition. Seven categories of uncertainties are considered: (1) jet energy scale, (2) initial state radiation, (3) final state radiation, (4) parton distribution functions, (5) the choice of Monte Carlo generator, (6) the top quark mass, (7) trigger and identification efficiencies and the luminosity. The relative strength of a systematic effect due to the source i is parameterized by the variable δ_i. Systematic effects influence the acceptance as well as the shape of the $Q \cdot \eta$ distribution. The $\pm 1\,\sigma$ changes in the acceptance of process j due an effect i are denoted by ϵ_{ij+} and ϵ_{ij-}; the numerical values of those parameters for the signal processes are given in Tab. III. The jet energy scale systematics is evaluated by applying energy corrections that describe ± 1-σ variations. ISR and FSR uncertainties are obtained from Monte Carlo samples where these effects were varied in Pythia showering such, that they represent ± 1-σ shifts. For the PDF uncertainty we checked several PDF sets and take the maximum deviation (MRST72) from our standard PDF set (CTEQ5L). The uncertainty associated with the choice of Monte Carlo generator we estimate by comparing to samples generated with TopRex [18]. We take half the difference between the acceptances calculated

from the MadEvent and the TopRex samples and assign this as a symmetric error. The uncertainties for jet energy scale and top-quark mass show clear asymmetries for positive and negative fluctuations. Those are a result of two window cuts we apply: (1) we use only the 2-jets bin in the W+jets spectrum and (2) we demand $140 \leq M_{\ell\nu b} \leq 210$ GeV/c^2, see Fig. 3a. Most shifts, positive as well as negative, tend to lower our acceptance because events are shifted out of these windows. For backgrounds most of the systematic uncertainties are absorbed into the cross-section (or rate) uncertainties Δ_j. Two major uncertainties are taken separately into account for the backgrounds: jet energy scale and top quark mass. For $t\bar{t}$ the uncertainties are $^{+25}_{-20}\%$ for jet energy scale and $\pm 4.4\%$ for the top mass. For the non-top background we use an uncertainty of $\pm 15.1\%$ for the jet energy scale in the separate search and $^{+10.1}_{-12.7}\%$ in the combined search. In total, the likelihood function $\mathcal{L}$ has 11 variables and is given by

$$\begin{aligned} L_s(\beta_1, \ldots, \beta_4; \delta_1, \ldots, \delta_7) \;=\; & \left\{ \prod_{k=1}^{B} \frac{e^{-\mu_k} \cdot \mu_k^{n_k}}{n_k!} \right\} \cdot \frac{e^{-\mu_d} \cdot \mu_d^{n_d}}{n_d!} \\ & \cdot \prod_{j=1,\, j\neq s}^{4} G(\beta_j, 1.0, \Delta_j) \cdot \prod_{i=1}^{7} G(\delta_i, 0, 1) \end{aligned}$$

where s denotes the signal process, which is $s-$ or t-channel, respectively. The μ_k are the mean number of events in bin k of the $Q \cdot \eta$ histogram, μ_d is the mean number of events in the double-tag bin. All variables except the signal cross-section β_s are considered nuisance parameters and are constrained to their expected values by Gaussian functions $G(x, x_0, \sigma_x)$. The parameters μ_k and μ_d are defined as follows:

$$\begin{aligned} \mu_k \;=\; & \sum_{j=1}^{4} \beta_j \cdot \nu_{j1} \cdot \left\{ \prod_{i=1}^{7} \left(1 + |\delta_i| \cdot (\epsilon_{ji+} H(\delta_i) + \epsilon_{ji-} H(-\delta_i))\right) \right\} \\ & \cdot \alpha_{jk} \cdot \left\{ \prod_{i=1}^{6} \left(1 + |\delta_i| \cdot (\kappa_{jik+} H(\delta_i) + \kappa_{jik-} H(-\delta_i))\right) \right\} \\ \mu_d \;=\; & \sum_{j=1}^{4} \beta_j \cdot \nu_{jd} \cdot \left\{ \prod_{i=1}^{7} \left(1 + |\delta_i| \cdot (\epsilon_{ji+} H(\delta_i) + \epsilon_{ji-} H(-\delta_i))\right) \right\}. \end{aligned}$$

Her ν_{j1} are the acceptances for process j in the 1-tag-bin. ν_{jd} is the acceptance in the double-tag-bin. The α_{jk} are the normalized template histograms, where j is the index of the process and k the bin number. The $\kappa_{jik+/-}$ are relative $\pm 1\,\sigma$ changes in the template

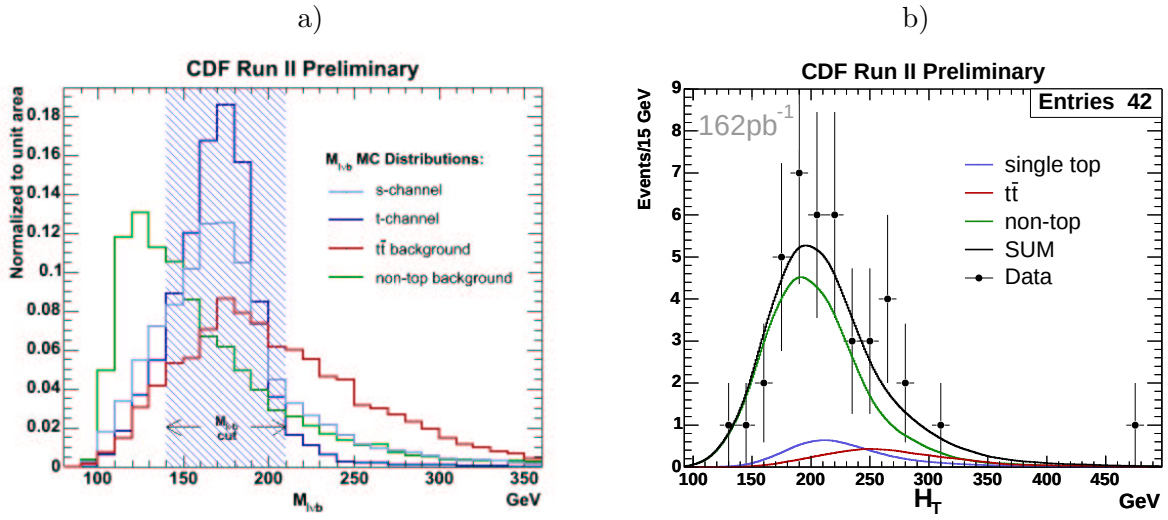

FIG. 3: a) $M_{\ell\nu b}$ distribution templates for Monte Carlo events. We show the optimized mass window cut. b) H_T distribution for data compared to the expectation.

histograms due to the systematic uncertainty i. H denotes the Heaviside function, needed to incorporate asymmetric errors. Systematic source number 7 comprises uncertainties due to the trigger efficiency, lepton identification efficieny, b-tagging efficiency and luminosity measurement, which are added in quadrature and define ϵ_{j7}. Since all these uncertainties contribute only to the normalization (the number of expected events), they do not change the template distribution and the κ_{j7k} are zero.

To measure the combined t- plus s-channel signal in our data (combined search), we use a kinematic variable whose distribution is very similar for the two single-top processes, but is different for background processes: the scalar sum H_T of $\not\!\!E_T$ and the transverse energies of the lepton and all jets in the event. For the combined analysis we use an analogous likelihood function as for the separate search. One difference is that in the combined search the H_T distributions were smoothed and yielded multi-bin histograms. The H_T distribution observed in data versus the SM expectation is shown in Fig. 3b.

To obtain the probability distribution $p(\beta_s)$ for the signal cross-section β_s, we first integrate out all nuisance parameters (i.e. all variables except β_s) from the likelihood function $L_s(\beta_1, \ldots, \beta_4; \delta_1, \ldots, \delta_7)$ and thereby construct the marginalized likelihood $L_s^*(\beta_s)$, which only depends on the signal cross-section β_s. When calculating the marginalized likelihood for the t-channel, the s-channel is treated as background and vice versa. $L_s^*(\beta_s)$ is normalized

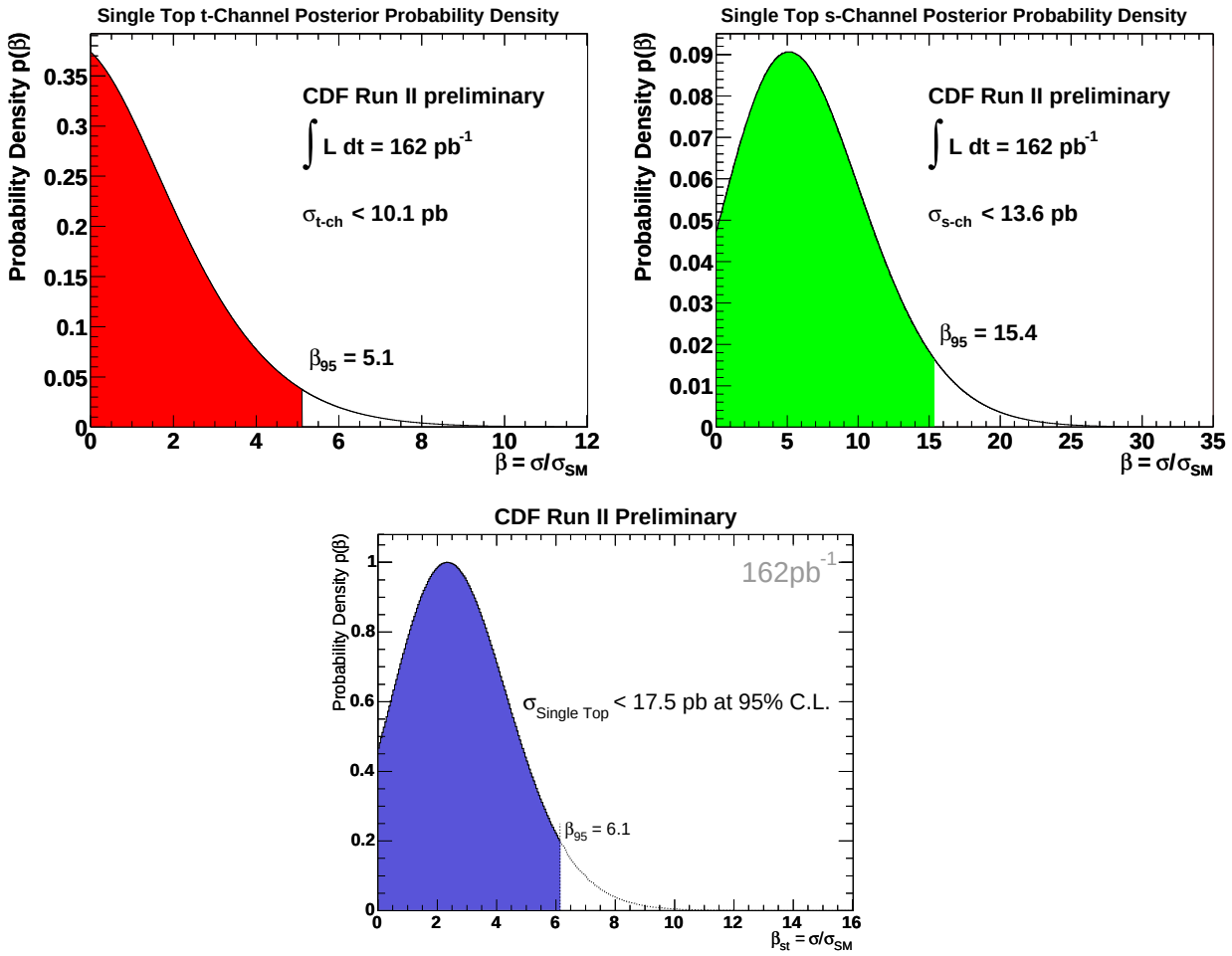

FIG. 4: Probability densities for signal cross-sections. The cross sections are normalized to their Standard Model prediction σ_{SM}.

and interpreted as probability density function $p(\beta_s)$ for the signal cross-section. To obtain a measure of our a-priori sensitivity we perform Monte Carlo experiments based on the signal cross-sections predicted by the Standard Model. For each experiment we calculate the 95% C.L. upper limit. We define the median of all Monte Carlo experiments as our sensitivity. We obtain $\sigma^{95}_{apriori} = 11.2$ pb ($\beta^{95}_{apriori} = 5.6$) for the t-channel, $\sigma^{95}_{apriori} = 12.1$ pb ($\beta^{95}_{apriori} = 13.7$) for the s-channel and $\sigma^{95}_{apriori} = 13.6$ pb ($\beta^{95}_{apriori} = 4.8$) for the combined search.

The resulting probability densities $p(\beta_s)$ for CDF II data are shown in Fig. 4. The maxima of the probability densities give the most probable values for the cross-sections. The maximum for the t-channel occurs at $\beta = 0.0^{+2.4}_{-0.0}$, for the s-channel at $\beta = 5.2^{+4.3}_{-4.3}$ and for the

combined signal at $\beta = 2.7^{+1.8}_{-1.7}$. The errors correspond to 1 σ confidence intervals. Since all these results are compatible with zero, we set upper limits on the single-top production cross section. To obtain the upper limit, we integrate the probability density from 0 to a value β^{95} for which the integral is 0.95. We call β^{95} the upper limit on the single-top cross-section at 95% confidence level (C.L.). For the t-channel we find an upper limit of 10.1 pb at 95% C.L. for the t-channel cross-section ($\beta^{95}_{t-ch} = 5.1$). For the s-channel we find an upper limit of 13.6 pb at 95% C.L. ($\beta^{95}_{s-ch} = 15.4$). For the combined search the upper limit is 17.8 pb at 95% C.L. ($\beta^{95}_{com} = 6.1$).

In summary, we could not establish evidence for electroweak single-top-quark production in (162 ± 10) pb^{-1} of data recorded with the Collider Detector at Fermilab. We set upper limits on the production cross-section, which are improved compared to previous Run I limits [7, 8]. Our results are the first limits set on single top production in Run II of the Tevatron, operating at a different center-of-mass energy. Another important aspect of our analysis are technical improvements, i.e. improved Monte Carlo for single top events and a fully Bayesian treatment of systematic errors in the likelihood function. These improvements will be important parts of future analayses aiming at the discovery of single-top quark production.

We wish to thank the Fermilab staff and the technical staffs of the participating institutions for their vital contributions. This work was supported by the U.S. Department of Energy and National Science Foundation; the Italian Instituto Nazionale di Fisica Nucleare; the Ministry of Education, Culture, Sports, Science and Technology of Japan; the Natural Sciences and Engineering Research Council of Canada; the National Science Council of the Republic of China; the Swiss National Science Foundation; the Bundesministerium für Bildung und Forschung, Germany; the Korean Science and Engineering Foundation and the Korean Research Foundation; the Particle Physics and Astronomy Research Council and the Royal Society, UK; the Russian Foundation of Basic Research; the Comision Interministerial de Ciencia y Tecnologia, Spain; in part by the European Community's Human Potential Program under contract HPRN-CT-20002; by the Research Fund of the Istanbul University Project No. 1755/21122001; by the Research Corporation.

We also wish to acknowledge the help of T. Stelzer (University of Illinois, Urbana) and S. Slabospitsky (Institute for High Energy Physics, Protvino) for the generation of MadEvent and TopRex Monte Carlo samples. We thank S. Mrenna and Z. Sullivan (both Fermilab)

for several useful discussions.

[1] S. Willenbrock and D.A. Dicus, Phys. Rev. D **34**, 155 (1986); S. Dawson and S. Willenbrock, Nucl. Phys. **B284**, 449 (1987); C.-P. Yuan, Phys. Rev. D **41**, 42 (1990); F. Anselmo, B. van Eijk and G. Bordes, Phys. Rev. D **45**, 2312 (1992); D. Carlson and C.-P. Yuan, Phys. Lett. B **306**, 386 (1993); G. Bordes and B. van Eijk, Nucl. Phys. **B435**, 23 (1995); T. Stelzer, Z. Sullivan and S. Willenbrock, Phys. Rev. D **56**, 5919 (1997); T. Stelzer, Z. Sullivan and S. Willenbrock, Phys. Rev. D **58**, 094021 (1998);

[2] S. Cortese and R. Petronzio, Phys. Lett. B **253**, 494 (1991); M.C. Smith and S. Willenbrock, Phys. Rev. D **54**, 6696 (1996); A.P. Heinson, A.S. Belyaev and E.E. Boos, Phys. Rev. D **56**, 3114 (1997); S. Mrenna and C.-P. Yuan, Phys. Lett. B **416**, 200 (1998).

[3] K. Hagiwara *et al.*, Phys. Rev. D **66**, 010001-113 (2002).

[4] B.W. Harris *et. al.*, Phys. Rev. D **66**, 054024 (2002).

[5] Z. Sullivan, Fermilba-Pub-04-142-T, hep-ph/0408049.

[6] G.L. Kane, G.A. Ladinsky and C.P. Yuan, Phys. Rev. D **45**, 124 (1992); D. Carlson, E. Malkawi and C.-P. Yuan, Phys. Lett. B **337**, 145 (1994); T.G. Rizzo, Phys. Rev. D **53**, 6218 (1996); E. Malkawi and T. Tait, Phys. Rev. D **54**, 5758 (1996); M. Hosch, K. Whisnant and B.-L. Young, Phys. Rev. D **56**, 5725 (1997); T. Tait and C.-P. Yuan, Phys. Rev. D **55**, 7300 (1997); E. Boos, L. Dudko and T. Ohl, Eur. Phys. J. C **11**, 473 (1999); T. Tait and C.-P. Yuan, Phys. Rev. D **63**, 014018 (2001); D. Espriu and J. Manzano, Phys. Rev. D **65**, 073005 (2002); E.H. Simmons, Phys. Rev. D **55**, 5494 (1997); P. Baringer, P. Jain, D.W. McKay and L.L. Smith, Phys. Rev. D **56**, 2914 (1997); C.X. Yue and G.R. Lu, Chin. Phys. Lett. **15**, 631 (1998); T. Han, M. Hosch, K. Whisnant, B.-L. Young, X. Zhang, Phys. Rev. D **58**, 073008 (1998).

[7] CDF Collaboration, D. Acosta *et al.*, Phys. Rev. D **65**, 091102 (2002).

[8] CDF Collaboration, D. Acosta *et al.*, Phys. Rev. D **69**, 052003 (2004).

[9] DØ Collaboration, V. Abazov *et al.*, Phys. Lett. B **517**, 282 (2001), Phys. Rev. D **63**, 031101 (2000).

[10] CDF Collaboration, FERMILAB-PUB-96/390-E (1996).

[11] D. Acosta *et al.*, Nucl. Inst. Meth. A **461**, 540 (2001), Nucl. Inst. Meth. A **494**, 57 (2002).

[12] CDF Collaboration, D. Acosta *et al.*, CDF 7132, submitted to Phys. Rev. D.

[13] T. Stelzer and W.F. Long, Phys. Commun. **81**, 337 (1994); F. Maltoni and T. Stelzer, hep-ph/0208156.

[14] T. Sjöstrand *et al.*, Comp. Phys. Commun. **135**, 238 (2001). We used the PYXTRA interface devised by S. Mrenna: `http://cepa.fnal.gov/personal/mrenna/generator.html`.

[15] R. Bonciani *et al.*, Nucl. Phys. B **529**, 424 (1998); M. Cacciari *et al.*, JHEP 0404:068 (2004), hep-ph/0303085.

[16] F. Caravaglios *et al.*, Nucl. Phys. B **539**, 215 (1999), hep-ph/9807570; M.L. Mangano, M. Moretti, R. Pittau, Nucl. Phys. B **632**, 343 (2002), hep-ph/0108069; M.L. Mangano *et al.*, JHEP 0307:001, (2003), hep-ph/0206293.

[17] J.M. Campbell and R.K. Ellis, *Update on vector boson pair production at hadron colliders*, Phys. Rev. D bf 60, 113006 (1999).

[18] S.R. Slabospitsky and L. Sonnenschein, Comput. Phys. Commun. 148 (2002) 87–102. hep-ph/0201292.